Conserved Scalar Measurements in Turbulent Diffusion Flames by a Raman and Rayleigh Ribbon Imaging Method

S. H. STÅRNER* and R. W. BILGER
Department of Mechanical Engineering, The University of Sydney, N.S.W. 2006, Australia

K. M. LYONS, J. H. FRANK, and M. B. LONG
Department of Mechanical Engineering, Yale University, P.O. Box 2157 Yale Station, New Haven, CT 06520-2157, USA

A new method to obtain images of conserved scalars in turbulent flames is presented and implemented with simultaneous Rayleigh and fuel Raman measurements in a methane/air jet diffusion flame by the use of a single dye laser and two intensified CCD cameras. The laser beam is focused to a line and retroreflected with a slight offset to form a thin ribbon, sufficient to measure gradients in two dimensions. A robust, iterative data reduction technique is used to derive statistics of temperature, fuel mass fraction, mixture fraction (f), and scalar dissipation (χ). Results for a flame of Reynolds number 20,600 show that the lower moments, pdfs, and scatter plots of the computed quantities do not differ markedly from published results of point measurements in similar flames, strengthening confidence in this new approach. The computed components of χ show behavior similar to that in nonreacting flows; there is some anisotropy, with the ratio of the radial to the axial component in the shear region around 2.0. The azimuthal component, measured by off-axis laser beam alignment, is roughly equal to the radial component. The correlation between f and χ is small on the flame axis, but the correlation coefficient $R_{f\chi}$ rises to around 0.4 near the edge, which is largely consistent with other recent results for cold jets and jet flames.

INTRODUCTION

This paper explores a new method of conserved scalar measurements in turbulent hydrocarbon diffusion flames, using joint fuel Raman/Rayleigh ribbon imaging, with the main aim of obtaining quantitative mixture fraction (f) and scalar dissipation ($\chi \equiv 2D\nabla f \cdot \nabla f$) statistics. The principles on which this method rests have been tested against full single-point Raman/Rayleigh measurements as regards the mixture fraction [1], but the gradient information collected in this work is new and as yet untested. The scarcity of other such flame data in the literature will confine validation largely to comparisons with cold flow results for the most vital statistics, such as the relationship between the components of χ and the joint probability density function (jpdf) of χ and f, aspects which bear directly on current modeling practice.

Other recent efforts in this direction include Rayleigh imaging in a H_2 flame at moderate Reynolds number [2], and Rayleigh imaging in cold flows [3, 4] from which deductions on flame structure have been made. Joint Rayleigh/fuel LIF imaging in an acetaldehyde flame [5–7] is a parallel effort to the present work; the acetaldehyde LIF intensity is orders of magnitude stronger than the spontaneous Raman scattering used here, and so lends itself easily to wide field two-dimensional imaging. However, there are queries regarding fuel pyrolysis and the effect of temperature on the LIF cross-section [7] that makes the more direct Raman measurement attractive despite its higher photon noise. Ribbon imaging, in which the laser line is broadened by retro-reflection is used here to optimize signal quality while preserving two dimensionality, so that two scalar gradient components may be measured.

Preliminary work [1] has shown that the diluted, piloted flame used here (3/1 air/methane by volume) is suitable for several reasons: it has been thoroughly documented by

*Corresponding author.
Presented at the Twenty-Fifth Symposium (International) on Combustion, Irvine, California, 31 July–5 August 1994.

Published by Elsevier Science Inc.

0010-2180/94/$7.00

point Raman/Rayleigh measurements [8, 9]; the air dilution reduces soot interference, widens the reaction zone, shifts the stoichiometric profile inside the shear layer, and, finally, increases the extinction Reynolds number.

Favre averaging (denoted by tilde overbar for the mean and " for the rms) is used in the presentation to make comparison with cold jet data more relevant. The results are presented mostly as radial profiles at the axial location $x/D = 25$ (where x is the distance from the nozzle and D the main jet nozzle diameter).

THE TWO-SCALAR METHOD

Stårner et al. [1] and Bilger [10] describe a method for mixture fraction mapping in two-stream reacting flows by two simultaneous scalar measurements. A brief outline of the theory and its application follows.

With the assumptions of homogeneous inlet conditions and unity Lewis numbers, we also simplify the kinetics to a one-step reaction between fuel F and oxidant O:

$$F + rO = (r + 1)P. \tag{1}$$

The fuel mass fraction Y_{fu} and the enthalpy $H = c_pT/Q$ are used to form the conserved scalar $\beta = Y_{fu} + c_pT/Q$. The mixture fraction f is then defined by

$$f \equiv \frac{\beta - \beta_2}{\beta_1 - \beta_2} = \frac{Y_{fu} + c_p(T - T_2)/Q}{Y_{fu,1} + c_p(T_1 - T_2)/Q}, \tag{2}$$

where subscripts 1 and 2 denote the fuel and air streams.

Rayleigh measurements are used to obtain temperature: $T = a_T/\mathrm{Ra}$, where Ra is the Rayleigh signal (corrected for laser energy variation) and the calibration factor a_T is proportional to the Rayleigh cross section of the mixture [1, 11]. Spontaneous Raman scattering from the fuel is the most direct method for obtaining Y_{fu}. With some manipulation, Eq. 2 can then be cast in a form which expresses the mixture fraction as a function of the Raman (Rm) and Rayleigh (Ra) measurements:

$$f = \frac{C_1 a_T}{W\,\mathrm{Ra}}\mathrm{Rm} + C_2 c_p(a_T/\mathrm{Ra} - T_2)/Q, \tag{3}$$

where C_1 and C_2 are constants, and W the mixture mole weight.

The appearance of a_T (proportional to the Rayleigh cross section σ), W, and c_p in Eq. 3, all of which are functions of f and the degree of reactedness, requires an iterative data reduction scheme: in the unreacted (frozen) mixture (subscripted '*fr*' below), σ and W vary linearly with the fuel concentration; in the "fully reacted" state both are nonlinear functions of f. Here we define the frozen state as that of fuel and oxidizer mixing without reaction, and the fully reacted state (subscripted '*r*') as that of predictions for an opposed flow laminar flame of the same composition, at a strain rate of 400 s^{-1}, around half of the extinction value, 810 s^{-1}. From these calculations tabulated outputs of $\sigma_r(f)$, $W_r(f)$, and $D(f)$, the molecular diffusivity of the mixture, are obtained. In Ref. 1, c_p/Q was taken as constant. Later work reveals that this restriction can be lifted owing to the iterative data reduction procedure. Here, a constant Q is computed, using Eq. 20 of Ref. 1 at stoichiometric as $Q = c_p(T_{ad} - T_2)/(f_s Y_{fu,1})$, with c_p the mean over the temperature range T_2 to T_{ad}. In the iterative procedure the value of c_p is a simple linear function of mixture fraction f and reactedness b: $c_p = [(1 - b)c_{p(\mathrm{frozen})} + bc_{p(\mathrm{burned})}]/2$, where the frozen and burned values are calculated for the local mixture fraction.

A potential source of error is inherent in the assumption of a one-step reaction: to the extent that the parent fuel is converted to intermediates in which the C–H bonds are broken, the Raman signal is lost. The laminar flame calculations can be used to quantify this effect: species such as CH_3 are assumed to contribute to the Raman signal in proportion to the number of C–H bonds per molecule and the number density. For methane this effect is small.

The reactedness b is defined here by $b = (T - T_2)/(T_r - T_2)$. In the iterative procedure, $\sigma = \sigma_{fr} + b(\sigma_r - \sigma_{fr})$. The mole weight and the diffusivity are computed similarly. A better approximation for the diffusivity would be $D = D_r(T/T_r)^{1.67}$. For each iteration, T, b, σ, c_p, and W are updated to yield an improved f. Convergence to within one percent normally occurs in less than four iterations. The fraction

of nonconverging nodes is typically 0.1 percent. Errors associated with the use of a single strain rate for the laminar flame calculations have been investigated [6]; the effect is very minor.

EXPERIMENTAL

The methane fuel is diluted with air (3/1 air/methane by volume) to eliminate soot. The stoichiometric value of f is 0.353. The fuel issues from a vertical nozzle of diameter D = 3.8 mm into a filtered, 6.5 m/s coflowing stream at Reynolds number 20,600, and has a small premixed annular pilot flame of H_2/C_2H_4/air. Pulses from a flash-lamp pumped dye laser (3 μs duration, 1 J, at 532 nm) provide the Rayleigh and the Raman signals. The horizontal beam is focused by a 150-mm focal length spherical lens to a 0.5-mm waist near the flame axis, and retro-reflected with a 0.5 mm vertical offset so that a very narrow ribbon, 1.0 mm high, is formed at the waist, sufficient to obtain axial gradients. The two opposed CCD cameras are fitted with lens-coupled intensifiers and $f/4$ (Rayleigh) and $f/1.2$ (Raman) collection optics, with 2/1 image reduction. An interference filter, 630-nm, 10-nm bandwidth, filters the Raman channel.

Soot precursor interference is found to be small at this axial location, affecting around 1% of the data. It can be reduced further in the iterative data reduction: by plotting fuel mass fraction versus temperature, corrupted data take non-physical values, well outside the completely reacted limit, and so can be identified and deleted.

Due to the intrinsic photon arrival statistics, the Raman channel has rather low signal-to-noise ratio (snr), typically $\approx$ 15. The optimal low-pass filtering to be applied would be such that the truncation of the Raman dissipation spectrum balances the residual noise after filtering. To estimate whether there is redundant spatial resolution in the measurements, the Kolmogorov length scale η has been calculated as follows: an integral length scale l is estimated using the measured half-radius L_f of f (in Fig. 1, L_f = 7.6 mm), setting the velocity half-radius L_u = Sc L_f (where Sc is the turbulent Schmidt number, Sc = 0.7) and l/L_u = 0.65 [12]; this yields l = 3.5 mm. (Alternatively,

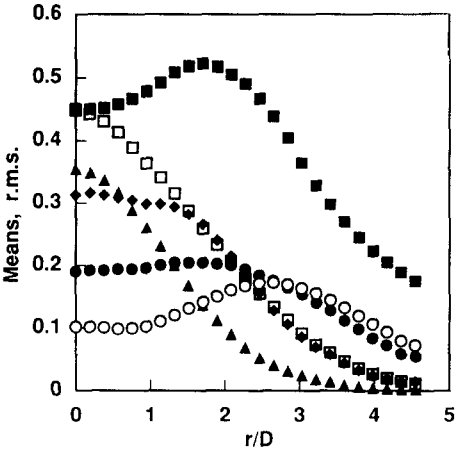

Fig. 1. Radial profiles of $\tilde{f}$(□); f''(●); $\tilde{Y}_{fu}$(▲); $Y''_{fu}/\tilde{Y}_{fu}$(◆); $\tilde{T}/2000$(■); $T''/2000$(○).

a measure of l can be obtained from the two-point correlation R_{11} in the radial direction: $l_r \equiv \int_0^\infty R_{11}\, dr$ yields l_r = 2.7 mm. This lower value is consistent with the observed anisotropy of the large scales in jet flames [13]. However in keeping with common practice where the integral length scale is typically derived from measurements in the axial direction, l = 3.5 mm is used below.)

The turbulence Reynolds number $\mathrm{Re}_t \equiv u'l/\nu$ is then estimated using velocity data by El-Banhawy et al. [14] for diluted CH_4 flames: u' = 7.2 m/s; ν is obtained from the known temperature profile; ν = 1.17 cm^2/s. This yields Re_t = 215 and $\eta = L_u\, \mathrm{Re}_t^{-3/4}$ = 0.095 mm. Tennekes and Lumley [15] estimate that the turbulence energy dissipation peak occurs at 30η, and that a resolution of 10η is adequate to capture the dissipation. Namazian et al. [16] estimate that around one half of the scalar dissipation energy is captured with a resolution of 10η. In the present work the resolution is 0.18 mm (twice the node spacing, by the Nyquist criterion), i.e., $\approx 2\eta$. The Raman signal dissipation spectrum $k^2E(k)$ peaks at wave number k ($\approx 2\pi/\lambda$) = 3.1/mm, corresponding to λ = 2 mm $\approx 20\eta$. It thus appears that there is room for low-pass filtering: a resolution of 5η (1/4 of the scale of the dissipation peak) should suffice; this is 2.6 times the resolution of the raw Raman data. We have chosen 3 × 3 pixel smoothing as this most closely corresponds to resolution 5η. Examina-

tion of the Raman dissipation spectrum $k^2E(k)$ shows that this filtering removes 21% of the energy content of the unfiltered data; two-thirds of the energy removed occurs at $\lambda < 5\eta$. The remaining third, representing $\sim 7\%$ of total energy, is presumed to be balanced to some extent by residual noise. The SNR of the filtered Raman data is ≈ 40, somewhat higher than that used in hardware probe measurement of χ in a plane jet [17].

RESULTS AND DISCUSSION

This section focuses in part on aspects of the Rayleigh/Raman method where difficulties may be expected; there are three areas of particular concern. Firstly, for fully burned fluid around stoichiometric ($f_s = 0.353$) composition, $Y_{fu} \approx 0$, so f is determined solely from the Rayleigh data which is at its minimum and may therefore lead to scatter at f_s. Secondly, the effect of soot precursor interference on the Raman data is known to peak slightly rich of f_s [18]. Finally, Raman noise and limited resolution are most noticeable in the scalar dissipation results and merit special attention.

Although mean and rms values of f, T, and Y_{fu} do not add new information to that already published [1], they are useful for testing the overall performance of the method. A comparison of the data in Fig. 1 (based on 500 images) with the point measurements by Masri et al. [19] shows similar values of the centerline fluctuation intensity $f''/\tilde{f}$ (here 0.185 at $25D$, versus 0.16 and 0.20 at $20D$ and $30D$, respectively) and the peak temperature fluctuation T'' (here 350 K at $25D$, versus 380 K and 520 K at $20D$ and $30D$). However, $Y''_{fu}/\tilde{Y}_{fu}$ is markedly higher (here 0.31 at $25D$, versus 0.17 and 0.22 at $20D$ and $30D$), indicating that Raman noise may have increased the measured fluctuation of Y_{fu}. However, the Raman signal contributes only in part to the computed mixture fraction, which can account for the fact that f'' is not correspondingly increased.

Radial profiles of mean and rms of the scalar dissipation components are shown in Fig. 2. The ratio of the radial to axial components, $\tilde{\chi}_r/\tilde{\chi}_x$, rises slightly from a minimum of 1.7 on the axis to 2.0 in the shear layer. This marked anisotropy, like very similar results for a plane

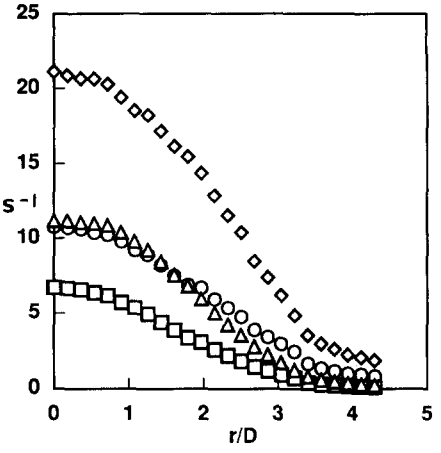

Fig. 2. Radial profiles of mean and rms of scalar dissipation components: $\tilde{\chi}_x$(□); χ''_x(○); $\tilde{\chi}_r$(△); χ''_r(◇).

air jet [17] and a round water jet [20], may be attributable to the moderate turbulence Reynolds number, 200 (160 for the plane air jet). The methane jet in Ref. 15, with $Re_t = 700$, shows very little anisotropy at $x/D = 17$. The ratio $\tilde{\chi}_{az}/\tilde{\chi}_r$ (where subscript az denotes the azimuthal component) has been measured at three off-axis radii; its value is near unity in the central region, peaks at 1.2 in mid shear layer and declines to unity at the outer edge. The common assumption that $\chi_{az} \approx \chi_r$ is thus fairly well supported by these results.

It can be seen in Fig. 2 that χ''_x and χ''_r are around twice the corresponding mean values, reflecting the local, very peaky distribution of χ. On the axis, the mean value of $\tilde{\chi}$ (here taken as $2\tilde{\chi}_r + \tilde{\chi}_x$) is 29 s^{-1}, so one can expect local fluctuations to exceed 200 s^{-1}. It is noteworthy that this range of χ (in this roughly half-extinguished flame) brackets the extinction value $\chi = 180$ s^{-1} (at stoichiometric) obtained by laminar flame calculations at strain rate 810 s^{-1}. At upstream locations in the turbulent flame, $x/D = 10$ and 20, peak values of χ are much higher; this is where extinction is known to be initiated [21].

The mixture fraction probability density functions (pdfs) in Fig. 3 show no marked anomaly around stoichiometric (the stoichiometric location is shown by vertical marks on the pdfs), indicating that any increase in scatter due to the minimum in the Rayleigh signal

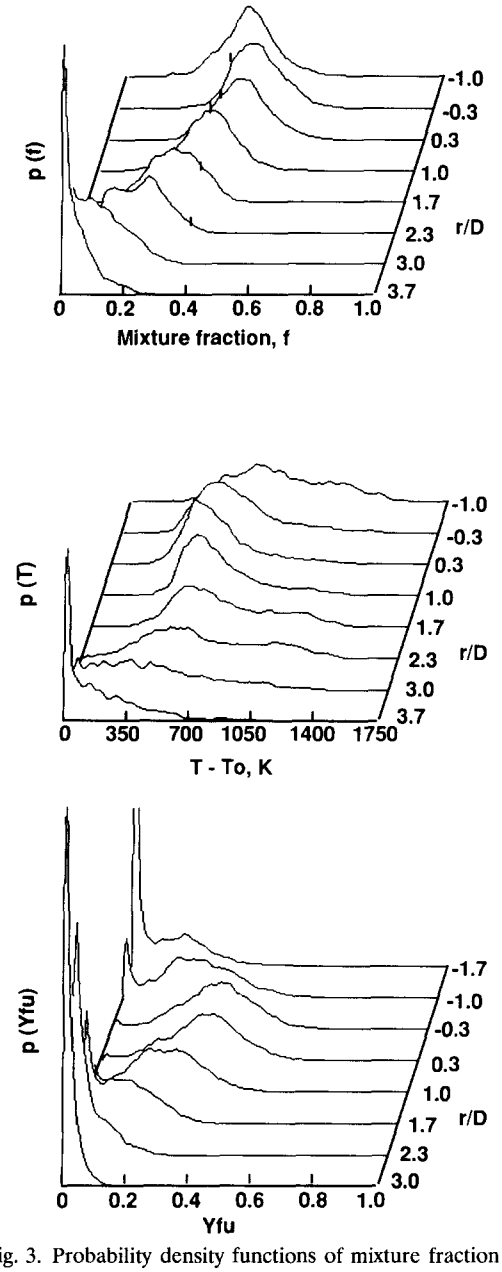

Fig. 3. Probability density functions of mixture fraction f, temperature T, and fuel mass fraction Y_{fu}. Negative values of r/D denote opposite side of flame axis.

near f_s is minor. The weak dual peaks in the pdf of f at $r/D = 2.3$ occur well lean of f_s; this appears to be a genuine manifestation of the turbulent-nonturbulent interface, smoothed by the superlayer. Similar weak dual peaks are found in the pdfs of f by Masri et al. [22]. In the pdf of the fuel mass fraction (Fig. 3), an intermittency spike is clearly seen.

The temperature pdf in Fig. 3 shows bimodality due to partial extinction: at $r/D = 2.3$ peaks tend to form around values for burned and unburned fluid. It is more clearly seen in Fig. 4 in the scatter plots of T and Y_{fu}, conditional on f: lean of f_s the distribution becomes bimodal. This phenomenon is amply documented elsewhere [9, 22]; the distributions in Fig. 4 are quite similar to those of the single

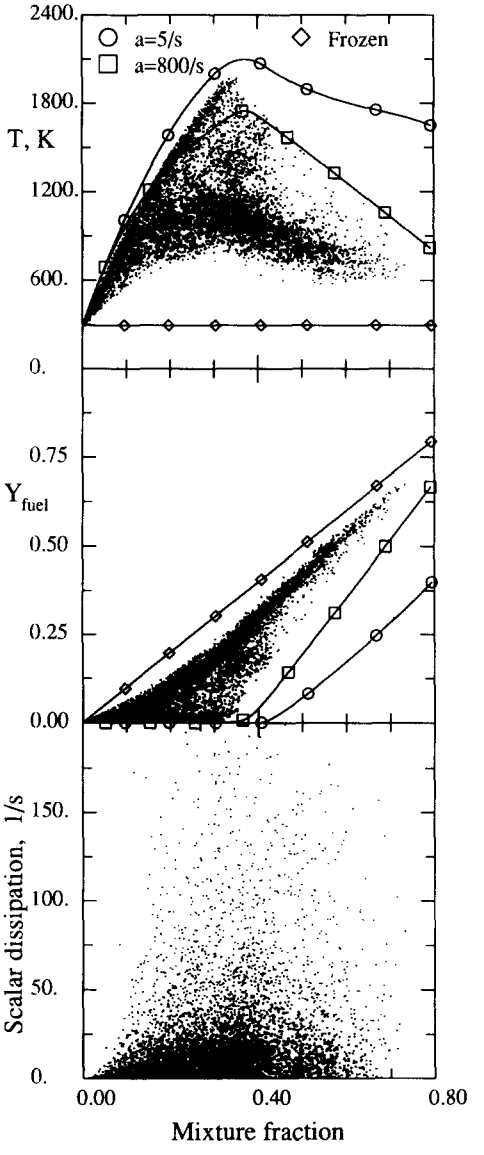

Fig. 4. Scatter plots of temperature, fuel mass fraction and scalar dissipation, conditional on mixture fraction with 8000 data points collected equally from all radii. Lines denote laminar flame calculations at strain rates 5 and 800 s^{-1}, and frozen flow.

point measurements, especially when it is taken into account that the present data cover a broader range of f than in Ref. 9. It can also be seen in Fig. 4 that there is no scatter of Y_{fu} outside the range of frozen to burned fluid.

The scatter plot of χ in Fig. 4 is based on the approximation that, instantaneously, $\chi_r = \chi_{az}$ so that $\chi = \chi_x + 2\chi_r$, as argued by Anselmet and Antonia [17]. However, it must be emphasized that this exaggerates the extrema of χ since χ_r and χ_{az} are not likely to have a strong positive correlation. The scatter plot of χ is more easily read when reworked as contours in Fig. 5; it is seen that the largest fluctuations in χ occur at, and just rich of, f_s. Figure 5 includes all data from $r/D = 0$ to 5, hence the peak at (0, 0).

Radial profiles of the important correlation between f and the components of χ are shown in Fig. 6. In common with results for a H_2 flame [2], the value of the correlation coefficient has a minimum on the axis and increases with radius. The results in Fig. 6 agree quite closely with those for a cold CH_4 jet [16] at $x/D = 17$. The dissipation of temperature (not a conserved scalar) in a lifted flame [23] seems more complex, but the range of the correlation coefficient at $x/D = 20$, -0.1 to 0.6, is similar. By contrast, for a plane air jet [17] the correlation seems very weak.

The simplifying assumption of independence of f and χ, which permits modeling of the jpdf

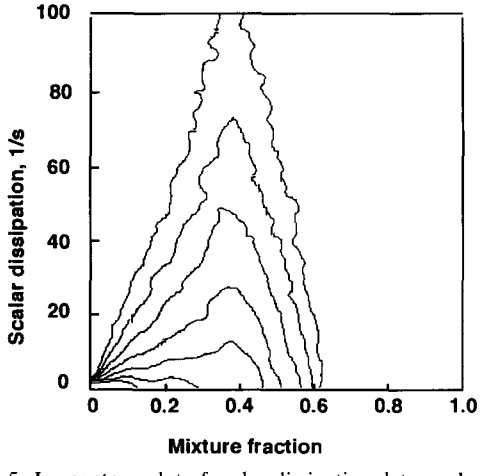

Fig. 5. Iso-contour plot of scalar dissipation data as shown in Fig. 5, but based on the full data set. Each contour is at twice the level of the one below.

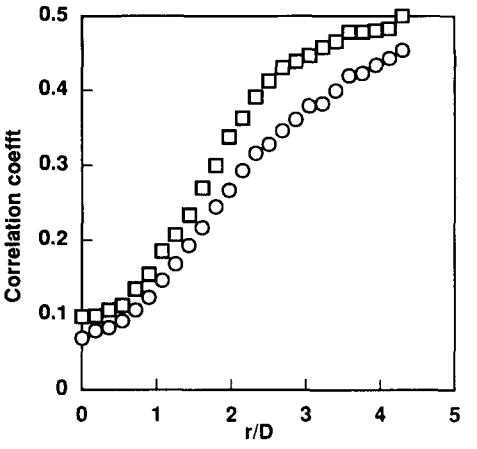

Fig. 6. Radial profile of the correlation coefficients between mixture fraction and the scalar dissipation rate components. Flame data as in Fig. 1. □: R_{fx_x}; ○: R_{fx_r}.

as the product of the two separate pdfs does not appear fully justified by these new results, but it should be noted that where the correlation is strong, χ and f are both small, so that the dependence overall is smaller than Fig. 6 suggests.

Of special interest for conditional moment closure modeling [24, 25] is the radial variation of the conditional scalar dissipation, $\langle \chi \mid f = \eta \rangle$, (conditional on f taking the value η), as shown in Fig. 7. For the less reacted fluid ($b < 0.5$) the modeling assumption that $\langle \chi \mid f = \eta \rangle$ is independent of radius seems tenable. For the more reacted fluid ($b > 0.5$) there is a marked increase with radius for data above stoichiometric composition. This increase may, however, be at least in part a measurement artifact: loss of Raman signal strength due to fuel pyrolysis at high temperature would artificially increase the mixture fraction gradient, and χ, just rich of stoichiometric. As there is also substantial scatter in the data in Fig. 7, the results for $b > 0.5$ must be viewed as tentative only.

CONCLUDING REMARKS

Realistic quantitative measurements of mixture fraction and scalar dissipation components have been obtained by two-scalar ribbon imaging. Comparison of the statistics of f, T, and Y_{fu} with the literature shows no marked

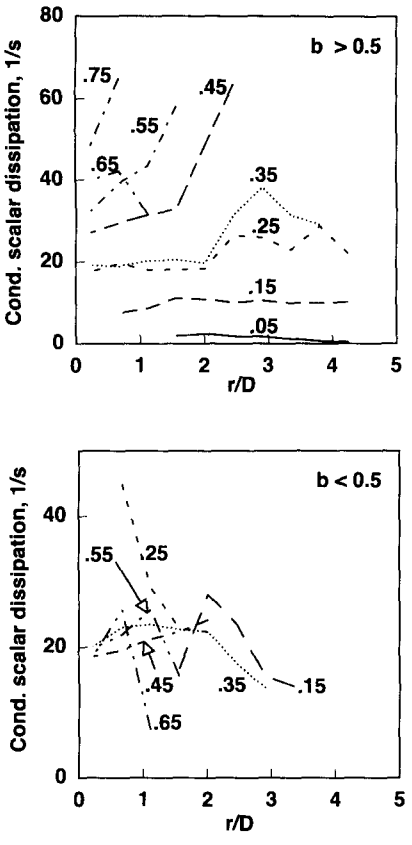

Fig. 7. Radial profiles, of conditional mean scalar dissipation, $\langle \chi \mid f = \eta \rangle$, conditional on the mixture fraction f taking the value η. Indicated on each graph are the midpoints of each interval in η; the interval size $\Delta\eta = 0.1$. Results are plotted separately for low and high reactedness ($b < 0.5$ and $b > 0.5$, respectively).

anomalies. Although little is as yet known about scalar dissipation statistics in jet flames, the results are consistent with the behavior one may expect from theory and by extrapolation from cold flow data. Simplifying assumptions, signal noise and limited spatial resolution all affect the results to some extent. However, the value of this method as a platform for further extensions, whereby measurements of radicals and/or velocity can be made jointly with f and χ, is so great for theory and modeling that the expense and complex equipment needed for such work is easily justified. Alternatives to the fuel Raman/Rayleigh combination are being investigated: fuel Raman/O_2 Raman is a viable combination when joint PIV measurements are considered, since the particle Mie scattering does not affect the filtered Raman data; the fuel Raman/N_2 Raman combination is attractive around stoichiometric, where N_2 is the one major species with strong signal and significant variation with f.

This work was supported in part by the Australian Research Council and the Air Force Office of Scientific Research under grant no. AFOSR-91-0150. The experiments were carried out at Yale University.

REFERENCES

1. Stårner, S. H., Bilger, R. W., Dibble, R. W., and Barlow, R. S., *Combust. Sci. Technol.* 86:223–236 (1992).
2. Stepowski, D., and Cabot, G., *Combust. Flame* 88:296–308 (1992).
3. Bilger, R. W., Yip, B., Long, M. B., and Masri, A. R., *Combust. Sci. Technol.* 72:137–155 (1990).
4. Buch, K. A., Dahm, W. J. A., Dibble, R. W., and Barlow, R. S., *Twenty-Fourth Symposium (International) on Combustion*, The Combustion Institute, Pittsburgh, 1993, p. 295.
5. Stårner, S. H., Kelman, J. B., Masri, A. R., and Bilger, R. W., *Proceedings of the Second International Symposium on Engineering Turbulence Modelling and Measurements*, Elsevier, Amsterdam, 1993.
6. Stårner, S. H., Bilger, R. W., Lyons, K. M., Marran, D. F., and Long, M. B., *Proceedings of the 14th International Colloquium on the Dynamics of Explosions and Reactive Systems*, Coimbra, Portugal, August 1993.
7. Long, M. B., Frank, J. H., Lyons, K. M., Marran, D. F., and Stårner, S. H., Paper 93-056 presented at the Western States Section meeting of the Combustion Institute, Menlo Park, Calif., October 1993.
8. Stårner, S. H., Bilger, R. W., Dibble, R. W., and Barlow, R. S., *Combust. Sci. Technol.* 70:111–133 (1990).
9. Stårner, S. H., Bilger, R. W., Dibble, R. W., and Barlow, R. S., *Combust. Sci. Technol.* 72:255–269 (1990).
10. Bilger, R. W., in *Experimental Methods in Combustion Flows* (A. M. K. P. Taylor, Ed.), Academic Press, 1993, pp. 1–51.
11. Driscoll, J. F., Schefer, R. W., and Dibble, R. W., *Nineteenth Symposium (International) on Combustion*, The Combustion Institute, Pittsburgh, 1983, p. 477.
12. Antonia, R. A., and Bilger, R. W., *J. Fluid Mech.* 61:805–822 (1973).
13. Schefer, R. W., Namazian, M., and Kelly, J., *Twenty-Second Symposium (International) on Combustion*, The Combustion Institute, Pittsburgh, 1989, p. 833.
14. El-Banhawy, Y., Hassan, M. A., Lockwood, F. C., and Moneib, H. A., *Combust. Flame* 53:145–148 (1983).
15. Tennekes, H., and Lumley, J. L., *A First Course in Turbulence*, The MIT Press, Cambridge, MA, 1973.

16. Namazian, M., Schefer, R. W., and Kelly, J., *Combust. Flame* 74:147–160 (1988).
17. Anselmet, F., and Antonia, R. A., *Phys. Fluids* 28:1048–1064 (1985).
18. Masri, A. R., Bilger, R. W., and Dibble, R. W., *Combust. Flame* 68:109–119 (1987).
19. Masri, A. R., Bilger, R. W., and Dibble, R. W., *Combust. Flame* 71:245–266 (1988).
20. Prasad, R. R., and Sreenivasan, K. R., *J. Fluid Mech.* 216:1–34 (1990).
21. Stårner, S. H., Bilger, R. W., Dibble, R. W., Barlow, R. S., Fourguette, D. C., and Long, M. R., *Twenty-Fourth Symposium (International) on Combustion*, The Combustion Institute, Pittsburgh, 1993, p. 341.
22. Masri, A. R., Bilger, R. W., and Dibble, R. W., *Combust. Flame* 73:261–285 (1988).
23. Boyer, L., and Queiroz, M., *Combust. Sci. Technol.* 79:1 (1991).
24. Klimenko, A. Y., *Fluid Dyn.* 25:327–334 (1990).
25. Bilger, R. W., *Phys. Fluids A* 5:436–444 (1993).

Received 22 November 1993; revised 16 April 1994